Ann. Rev. Fluid Mech. 1984. 16:99–137

NUMERICAL SIMULATION OF TURBULENT FLOWS[1]

Robert S. Rogallo and Parviz Moin

Computational Fluid Dynamics Branch, NASA Ames Research Center, Moffett Field, California 94035

1. INTRODUCTION

A century has passed since O. Reynolds demonstrated that fluid flow changes from an orderly and predictable state to a chaotic and unpredictable one when a certain nondimensional parameter exceeds a critical value. The chaotic state, turbulence, is the more common one in most flows at engineering and geophysical scales, and its practical significance, as well as the purely intellectual challenge of the problem, has attracted the attention of some of the best minds in the fields of physics, engineering, and mathematics. Progress toward a rigorous analytic theory has been prevented by the fact that turbulence dynamics is stochastic (often having underlying organized structures) and strongly nonlinear. There are, however, rigorous kinematic results that stem from tensor analysis and the linear constraint of continuity, and these allow a reduction of variables in the statistical description of the velocity field in certain cases, especially for isotropic turbulence. Rigorous dynamical results are available only for limiting cases where the governing equations can be linearized, and although the required limits are seldom approached in practice, the linear analysis provides guidance for model development. In spite of the dearth of rigorous nonlinear results, we have accumulated over the years a surprisingly good qualitative understanding of turbulence and its effects. Indeed, the gems of turbulence lore are the scaling laws for particular domains (either in physical or wave space), which result from the recognition of the

[1] The US Government has the right to retain a nonexclusive royalty-free license in and to any copyright covering this paper.

essential variables and the constraint of dimensional invariance. In particular, the Kolmogorov law, and the law of the wall, are so well established that compatability with them is required of any theory or simulation.

All attempts at a statistical theory of turbulence have ultimately been faced with the problem of closure, that is, the specification at some order of a statistical quantity for which no governing equation exists. The success of the closure model depends not only on the flow configuration, but also on the statistical order at which results are desired. When the closure model is inadequate for accurate determination of the desired statistics, the model must be improved, or closure postponed to yet higher order. Most of the closures attempted to date may be classified as either one-point or two-point, depending on the number of spatial points appearing in the desired statistical results. Reviews of the many one-point closures are given by Reynolds (1976) and Lumley (1980). The much more complicated two-point closures [the Direct Interaction Approximation (DIA) and the related Test Field Model (TFM) of Kraichnan (see Leslie 1973), and the Eddy Damped Quasi-Normal Markovian (EDQNM) model of Orszag (1970), Lesieur & Schertzer (1978), and Cambon et al. (1981)] have been limited to homogeneous (usually isotropic) flows, where symmetry allows a reduction of variables.

Progress in the experimental study of turbulence has not been as difficult as that of analysis, but it has required great ingenuity in the collection of data and often in setting up the flows themselves. The results are usually of two kinds: statistical and visual. The velocity statistics are collected by use of hot-wire probes and, more recently, also by use of the laser Doppler velocimeter. Flow visualization has been particularly useful in aiding the interpretation of statistical data and identifying persistent flow structures. The primary difficulty with experimental turbulence data is the lack of it; the theoretician needs a number of statistical quantities, some of which (for example, those involving the pressure) are difficult to measure. A secondary problem is the isolation of the effect of a single parameter; for example, the effect of rotation on the decay of turbulence generated by a screen in a wind tunnel must be separated from the effect of rotation on the turbulence-generation process itself. Modern electronic recording and computing equipment has increased the quantity and quality of available data and has led to more-sophisticated analysis techniques (for example, conditional averages and pattern recognition).

The turbulence problem is so challenging that any research tool found successful in even remotely similar problems is quickly brought to bear. The two-point closures are such examples, as are the concepts of "critical phenomena," "strange attractor," and "renormalization." The high-speed

digital computer is another recently developed tool with obvious application to the problem. The computer is used in other ways in fluid dynamics (see Van Dyke's article in this volume), but its most straightforward use is for "brute force" numerical simulation.

The numerical simulation of turbulence as we know it today rests largely on foundations laid down by the meteorologists at the National Center for Atmospheric Research (NCAR); their early work is reviewed by Fox & Lilly (1972). Since that time, computer capacity has increased by over an order of magnitude as has the number of workers in the field. Although some progress has been made in the efficiency and accuracy of computational algorithms, particularly in the adaptation of spectral methods, the primary pacing item determining our ability to simulate turbulence is the speed and memory size of the computing hardware (Chapman 1979, 1981).

The choice between simulation and experiment for a specific flow reduces to two questions: can the desired data be obtained at the required accuracy, and if so, how much will it cost? At the present time, simulation can provide detailed information only about the large scales of flows in simple geometries, and is advantageous when many flow quantities at a single instant are needed (especially quantities involving pressure) or where the experimental conditions are hard to control or are expensive or hazardous. Simulation cannot provide statistics that require a very large sample or that remain sensitive to Reynolds number even at high Reynolds number. It is particularly advantageous to use both simulation and experiment for delicate questions involving stability or sensitivity to external influences.

Turbulence consists of chaotic motion, and often persistent organized motions as well, at a range of scales that increases rapidly with Reynolds number. This restricts complete numerical resolution to low Reynolds number. When the scale range exceeds that allowed by computer capacity, some scales must be discarded, and the influence of these discarded scales upon the retained scales must be modeled. We shall distinguish between completely resolved and partly resolved simulations by referring to them as "direct" and "large-eddy" (LES), respectively, although these terms are often used interchangeably in the literature to indicate both without distinction. The descriptor "large-eddy" is misleading when the important flow structures to be resolved are extremely small as are those near solid boundaries, and at the dissipation scale at high Reynolds number. The attraction of direct simulation is that it eliminates the need for ad hoc models, and the justification often advanced is that the statistics of the large scales vary little with Reynolds number and can be found at the low Reynolds numbers required for complete numerical resolution. This approach has been successful for unbounded flows where viscosity serves mainly to set the scale of the dissipative eddies, but it has not been successful

for wall-bounded flows, such as the channel flow, where computational capacity has so far not allowed a Reynolds number at which turbulence can be maintained. This is typical of many flows of engineering interest and forces the development of the LES approach.

The basic philosophy of LES is to explicitly compute only the large-scale motions that are directly affected by the boundary conditions and are therefore peculiar to the problem at hand. The small-scale motion is assumed to be more nearly universal, that is, its statistics and their effect upon the large scales can be specified by a small number of parameters. We hope that convergence of the method with increasing resolution will be rapid, because our ability to parameterize the sub-grid scale (SGS) effects should improve as the SGS length and time scales become disparate from those at energetic scales, and also simply because the SGS effects are proportional to the reduced SGS energy. The LES approach lies between the extremes of direct simulation, in which all fluctuations are resolved and no model is required, and the classical approach of O. Reynolds, in which only mean values are calculated and all fluctuations are modeled.

The numerical simulation of turbulence requires judgments with respect to the governing equations, initial and boundary conditions, and numerical resolution and methods. In the following sections we discuss some of the available choices and the results that follow from them.

2. GOVERNING EQUATIONS

We limit our discussion of simulation technique to flows of incompressible Newtonian fluids governed by the Navier-Stokes equations. Effects of buoyancy, compressibility, density stratification, magnetic forces, and passive scalar transport introduce new physical phenomena but increase the simulation difficulty in degree rather than kind. The convective terms of the equations produce a range of scales limited by molecular diffusion, so that with sufficiently low Reynolds number the entire range can be numerically resolved and no modification of the governing equations is required. When computer capacity does not allow complete resolution and the equations are not modified to take this into account, the computed values may have no relation to fluid physics. The numerical algorithm may become unstable as the smallest computed scales accumulate energy or, when energy-conserving numerical approximations are used, the energy may reach a nonphysical equilibrium distribution among the finite degrees of freedom. Orszag (see Fox & Lilly 1972) has demonstrated that energy-conserving numerics in inviscid isotropic flow lead to energy equipartition among the degrees of freedom, and this is often used as a check of algorithms and programming in simulation codes. When the viscosity is not

zero but is too small to allow accurate resolution of the dissipation scales, an energy-conserving algorithm collects energy at the smallest computed scales until the dissipation and cascade rates reach equilibrium. Kwak et al. (1975) show that this excess energy, trapped at the mesh scale rather than cascading to the Kolmogorov scale, produces too rapid an energy transfer from large scales. This would be expected if the small scales act on the large scales as an eddy viscosity with a value, proportional to the length and velocity scales of the trapped energy, that is increased by the entrapment. One of the most important modifications of the Navier-Stokes equations is a mechanism for removal of energy from the computed scales that mimics as closely as possible the physical cascade process. The first step in an LES is then to define the variables that can be resolved and their governing equations.

The values at discrete mesh points of a simulation represent flow variables only in some average sense, and one way to define this sense is to find the differential equations that are exactly equivalent to the discrete approximation of the Navier-Stokes equations (Warming & Hyett 1974). The popular second-order central difference formula for the derivative of a continuous variable, for example, gives exactly the derivative of a second continuous variable that is an average of the first one:

$$\frac{u(x+h)-u(x-h)}{2h} = \frac{d}{dx}\left\{\frac{1}{2h}\int_{x-h}^{x+h} u(\xi)\,d\xi\right\}. \tag{1}$$

This shows how a discrete operator filters out scales less than the mesh size h. The direct use of such operators on the terms of the Navier-Stokes equations then introduces a different averaged variable for each term, depending on the derivative and discrete operator involved. This direct approach is therefore limited to completely resolved flows where the averages cause no information loss and all such averages give the same value. When the Reynolds number is too high for the direct approach, the range of scales can be limited to a resolvable size by explicitly filtering the Navier-Stokes equations. This formally defines the averaging process that separates resolvable from subgrid scales and the SGS stresses that must be modeled. When the smallest scale, $O(\Delta)$, allowed by the filter and the SGS model is sufficiently greater than the smallest scale, $O(h)$, resolved by the mesh, the results of the computation are independent of the choice of numerical algorithm and depend only on the filter and SGS model. Complete separation of physics from numerics is very costly in an LES, where mesh doubling in three directions increases the cost by an order of magnitude or more and in practice $\Delta = O(h)$ in each direction. Thus, resolution of the smallest computed scales is often marginal, and care is required to insure that the truncation error is less than the physical SGS

effects. Leonard (1974) applies the homogeneous filter

$$\bar{f} = \int_{-\infty}^{+\infty} G(\mathbf{x}-\boldsymbol{\xi}) f(\boldsymbol{\xi})\, d\boldsymbol{\xi}, \qquad f = \bar{f} + f' \tag{2}$$

to the Navier-Stokes equations to obtain the "resolvable-scale" equations

$$\begin{aligned} &\frac{\partial \bar{u}_i}{\partial t} + \frac{\partial}{\partial x_j}\overline{u_i u_j} + \frac{1}{\rho}\frac{\partial \bar{p}}{\partial x_i} = \nu \nabla^2 \bar{u}_i, \\ &\frac{\partial \bar{u}_i}{\partial x_i} = 0. \end{aligned} \tag{3}$$

Here, and throughout the paper, an overbar denotes a resolvable scale quantity and a prime denotes an SGS quantity. The convective fluxes are

$$\overline{u_i u_j} = \overline{\bar{u}_i \bar{u}_j} + Q_{ij}, \qquad Q_{ij} = \overline{\bar{u}_i u_j'} + \overline{u_i' \bar{u}_j} + \overline{u_i' u_j'}. \tag{4}$$

The equations must be closed by specifying these fluxes as functionals of the resolved variables. The terms containing u' must be modeled, but only the deviation from isotropy has dynamic effect. The $\bar{u}_i \bar{u}_j$ term may be computed directly from resolved variables. When the average is uniform over an unbounded homogeneous dimension (space or time) or is a statistical (ensemble) average, the postulates of O. Reynolds lead to $\overline{u_i u_j} = \bar{u}_i \bar{u}_j + \overline{u_i' u_j'}$, but the postulates do not apply to averages over bounded domains (Monin & Yaglom 1971, Leonard 1974). The convolution (2) simplifies to $\bar{f}(\mathbf{k}) = G(\mathbf{k}) f(\mathbf{k})$ in wave space, from which it follows that $\overline{f'} = G(1-G)f$ is zero only when G is piecewise constant at values of 0 or 1. Reynolds' average is equivalent to $G(\mathbf{k}) = 0$ for $|\mathbf{k}| > 0$, and Fourier spectral methods implicitly filter with $G(\mathbf{k}) = 0$ for $|\mathbf{k}| > k_{\max}$. In the latter case $\overline{\bar{u}_i \bar{u}_j} = \bar{u}_i \bar{u}_j$ for resolved $\mathbf{k}$, but $\overline{\bar{u}_i u_j'} \neq 0$ there.

An alternative derivation of the resolvable scale equations by Schumann (1975) averages the equations over the cell volumes of a fixed mesh. This leads directly to the integral form of the Navier-Stokes equations in which time derivatives of cell-volume velocity averages are related to differences of cell-surface average stress and momentum flux. The various surface averages of momentum flux are decomposed as in (4) assuming Reynolds postulates, and the required surface averages of velocity and its gradient are related to volume averages of velocity by Taylor-series expansion. There is an inconsistency between the assumption of piecewise constant velocity required for validity of the Reynolds postulates and the use of Taylor-series expansions, but the resulting equations, except for the SGS model, are precisely those obtained by Deardorff (1970) using the continuous averaging process (1) and second-order numerics on a staggered uniform mesh.

The cell-volume averaging used by Deardorff and Schumann does not satisfy Reynolds postulates, and the difference $\overline{u_i u_j} - \bar{u}_i \bar{u}_j$ is modeled. The part of this, $\overline{\bar{u}_i \bar{u}_j} - \bar{u}_i \bar{u}_j$, that can be computed directly from resolved variables is known as the Leonard term. Leonard (1974) shows that this term removes significant energy from the computed scales and should probably not be lumped with the SGS terms. If direct calculation of the term is difficult he proposes a simple model, based on its Taylor-series expansion:

$$\overline{\bar{u}_i \bar{u}_j} \sim u_i u_j + \frac{\gamma}{2} \nabla^2 (u_i u_j) + \cdots, \qquad \gamma = \int_{-\infty}^{+\infty} |\xi|^2 G(\xi)\, d\xi. \tag{5}$$

At low Reynolds number Clark et al. (1979) find this form to be quite accurate when compared with values from a direct simulation. Shaanan et al. (1975) used a numerical operator for the divergence of the flux tensor in the Navier-Stokes equations that has lowest-order truncation error of nearly the form (5), thereby implicitly capturing the Leonard term. Most subsequent authors who explicitly filter the equations simply compute $\overline{\bar{u}_i \bar{u}_j}$ (Mansour et al. 1979). Clark et al. (1977) also find that the measured "cross" terms $C_{ij} = \overline{\bar{u}_i u_j'} + \overline{u_i' \bar{u}_j}$ drain significant energy from the resolved scales. Again, part of the effects can be captured by a Taylor-series expansion of the *resolved scale* velocity:

$$\overline{\bar{u}_i' \bar{u}_j} \sim \overline{\bar{u}_i'} \bar{u}_j + \frac{\Delta^2}{12} \frac{\partial \overline{\bar{u}_i'}}{\partial x_k} \frac{\partial \bar{u}_j}{\partial x_k} + \cdots, \tag{6}$$

where $\overline{\bar{u}_i'} = \bar{u}_i - \bar{\bar{u}}_i$, and we have used a Gaussian filter, $G(\xi) = \sqrt{(6/\pi\Delta)}\, e^{-6\xi^2/\Delta^2}$. Clark et al. (1977) propose a different model for the cross terms, but its derivation involves the Taylor-series expansion of the SGS velocity field. The dependence of the modeled terms in (4) upon the filter (for example, the vanishing Leonard term for sharp filters in wave space) suggests that simulation accuracy might be improved by a particular choice. Deardorff (1970) and Schumann (1975) use cell-volume averages related as in (1) to their finite-difference operators, and Chollet & Lesieur (1981) use the sharp filter implied by their Fourier spectral methods. When the choice of filter is divorced from the numerical algorithm, and this can only occur for $\Delta \gg h$, the Gaussian filter (Kwak et al. 1975, Shaanan et al. 1975, Mansour et al. 1978, Moin & Kim 1982) is usually used for homogeneous dimensions because it provides a smooth transition between resolved and subgrid scales and is positive definite (in fact Gaussian) in both physical and wave space. The optimum choice is of course the combination of filter and model that minimizes the total simulation error. The ratio of

filter to mesh resolution, Δ/h, serves primarily to control numerical error, while the form of the filter and the form of the closure model determine the modeling error. The dependence of the model on the filter is studied, in isotropic flow within the TFM framework, by Leslie & Quarini (1979) and, for solutions of the Burgers equation, by Love (1980).

The averaged Navier-Stokes equations (3, 4) provide a conceptual framework for the discussion of modeling. The practical value of explicitly filtering the convective terms is a matter of current debate. The Leonard term is $O(\Delta^2)$, so it seems pointless to compute it separately in simulations using second-order numerics with error of $O(h^2)$ unless $\Delta/h \gg 1$ and the filtered field is well resolved. When the Leonard term is not swamped by numerical error, the filter, SGS stresses, and velocity field are related by (4), and the filter and model, $M(u)$, should in principle be selected together to minimize in some sense the modeling error $\overline{u_i u_j} - \overline{\bar{u}_i \bar{u}_j} - M_{ij}(\bar{u})$; the filtered convection $\overline{\bar{u}_i \bar{u}_j}$ is then computed directly. Kwak et al. (1975), for example, assume a Gaussian filter and a Smagorinsky (1963) SGS model and optimize the filter width and model constant by matching decay rate and spectral shape from the LES with experimental data for isotropic turbulence. A general study of filter and model forms has not yet been attempted. But the true filter is always uncertain because of the inherent inability of SGS models to exactly satisfy (4), so that the Leonard term cannot be found without error. An argument against separate treatment of the Leonard term is advanced by Antonopoulos-Domis (1981), who finds that in his LES calculations it moved energy from the small resolved scales to the large ones, rather than to the subgrid scales as predicted by Leonard. Leonard & Patterson (unpublished) point out that in isotropic turbulence the transfer spectrum $T(k)$ associated with the flux $\bar{u}_i \bar{u}_j$ is negative at small k, positive at large k, and is conservative. The transfer spectrum associated with the filtered flux $\overline{\bar{u}_i \bar{u}_j}$ is simply $G(k)T(k)$ and can reasonably be expected to remove energy from the resolved scales. The proper way to determine the effect of the Leonard term is to measure the energy transfer associated with the filtered convective term in an *accurately resolved field*. Studies of this kind by Leonard & Patterson, Clark et al. (1979), and Leslie & Quarini (1979) have verified the energy drain but at a lower magnitude than Leonard's original estimate. Antonopoulos-Domis draws his conclusions from simulations with no viscous or modeled turbulent terms. His results do indicate that the approximate form (5) alone is not sufficient to stabilize the calculation, but they do not indicate the effect of the Leonard term in a well-resolved calculation. A more general problem with explicit filters is the difficulty of extending them to inhomogeneous dimensions, where differentiation and filtering do not in general commute, but this does not seem insurmountable.

The equations of LES are then essentially the original Navier-Stokes equations written for averaged variables, with a filtered convection term and additional terms to model the effects of the unresolved scales. The only change from the original analysis of O. Reynolds is the use of averages over bounded domains, which requires the convective term to be filtered. The crux of the problem remains the closure model.

3. MODELS

Statistical homogeneity in space or time reduces the dimensions of the Reynolds-averaged problem, and all of the effects of fluctuations in the missing dimensions must be accounted for by the model. The variation of correlations in the remaining inhomogeneous dimensions is peculiar to the specific problem and cannot be modeled in a universal way. In an LES the equations are averaged over only small scales and retain all space-time dimensions. The averaging process is chosen to resolve numerically the physical features of interest, and the desired statistics are measured directly from the computed scales. The role of the model is not to provide these statistics directly, but to prevent the omission of the unwanted scales from spoiling the calculation of scales from which statistics are taken.

It is apparent from the LES work to date that the most important contribution of the model is to provide, or at least allow, energy transfer between the resolved and subgrid scales at roughly the correct magnitude. This transfer is usually from resolved to subgrid scales but may be reversed near solid boundaries, where the small productive eddies are not resolved and the SGS model must account for the lost production. Models can be tested either by directly comparing the modeled quantity with the model itself, using data from a reliable source (theory, experiment, or direct simulation), or by using the model in an LES and comparing results with those from a reliable source. The detailed information required for the former test can be supplied only by theory or simulation, and in practice the latter procedure is the more common. This is consistent with the LES philosophy; the model is not required to supply detailed information about the subgrid scales. But there is frequently a need to improve the model's description of physical detail and thus allow increased reliance on the model and lower computation cost. The sequence of model complexity could follow the same path as for the Reynolds-averaged equations, with the introduction of separate equations for the SGS stress or energy (Deardorff 1973). But in an LES the SGS length scales are given by the filter width, and velocity scales can be estimated from the smallest resolved scales. Bardina et al. (1980) suggest that the SGS stresses themselves be modeled by an extrapolation of the computed stresses at the smallest

resolved scales. The simplest model, $\overline{u_i'u_j'} \sim C\overline{u_i'}\,\overline{u_j'} = C(\bar{u}_i - \bar{\bar{u}}_i)(\bar{u}_j - \bar{\bar{u}}_j)$, has been tested by McMillan et al. (1980) using data from direct simulations. The model correlates much better with the data than does a typical eddy-viscosity model, but Bardina et al. find that it is not sufficiently dissipative to stabilize an LES.

The effects of discarded scales on computed ones consist of "local" contributions, which diminish rapidly as the interacting scales are separated, and "nonlocal" contributions, which are significant even for widely separated scales. The interaction between scales of similar size retains the full complexity of the original turbulence problem, so there is little hope of modeling the local effects well. On the other hand, interaction of disparate scales is easier to analyze, so that nonlocal effects can be modeled with greater confidence.

The modern statistical theories of isotropic turbulence (DIA, TFM, EDQNM) provide models in which the roles of the various scales can be determined. Kraichnan (1976) and Leslie & Quarini (1979) evaluate the transfer spectrum within the TFM model, showing explicitly the local and nonlocal (in wave space) effects of the truncated scales on the energy flow within the resolved scales. The transfer spectrum is of the form $T(k) = -2\nu(k)\sqrt{E(k_m)/k_m}\,k^2E(k) + U(k)$, where k is the wave-number magnitude, k_m is the limit of wave-number resolution, $\nu(k)$ is a nondimensional eddy viscosity, and E is the three-dimensional energy spectrum. The first term arises from stresses like $\overline{\bar{u}_i u_j'}$, while the "backscatter" term $U(k)$ arises from the $\overline{u_i'u_j'}$ stresses. The forms $\nu(k)$ and $U(k)$ depend upon both the filter and the energy spectrum; Kraichnan considers a sharp k filter in an infinite inertial subrange, and Leslie & Quarini extend these results to a Gaussian filter and more-realistic spectra. Kraichnan finds that the local effects are confined to scales within an octave of k_m and are characterized by a rapid rise in transfer as k approaches k_m. The net energy flow across k_m is dominated by this local transfer as described by Tennekes & Lumley (1972). Below this local range, $k < k_m/2$, the viscosity is independent of k [but depends on time through $E(k_m)$], and the backscatter decays like k^4 (Lesieur & Schertzer 1978). This backscatter might be important in unbounded flows, where length scales grow indefinitely and, as Leslie & Quarini note, its form is not well represented by an eddy-diffusion model because neither its magnitude nor anisotropy level are set by the large scales. Their results indicate that a Gaussian filter damps the SGS contribution to the local cascade too severely and broadens its range; this suggests that a sharper filter might be found in which the Leonard term carries the entire local transfer and leaves only the nonlocal effects to be modeled. Chollet & Lesieur (1981) achieve the same end using Kraichnan's effective eddy viscosity to successfully close both EDQNM and LES calculations. Chollet (1982) closes an LES by

coupling it to an EDQNM calculation for the effective eddy viscosity, thus avoiding an assumed SGS energy spectrum. This is a rather elaborate "one-equation" model. The extension of EDQNM to homogeneous anisotropic flows by Cambon et al. (1981) allows application of this approach to less-restricted SGS stresses, but at a great increase in complexity. Yoshizawa (1979, 1982) relates these statistical closures in wave space to the gradient-diffusion closures in physical space by a formal multiscale expansion. The assumption that the SGS time scale, as well as space scales, is disparate from those of the resolved scales leads to SGS stresses that are locally isotropic at lowest order and of gradient-diffusion form (scalar eddy viscosity) at next order. The more interesting limit of commensurate time scales, leading to homogeneous but anisotropic SGS turbulence at lowest order, is prevented by the resulting complexity of the required DIA closure.

The gradient-diffusion model for SGS stresses is usually postulated with appeal to the similar stresses produced by molecular motion. But it is well known (Tennekes & Lumley 1972, Corrsin 1974) that the required scale separation, present in the case of molecular diffusion, does not occur between all of the scales of turbulence. In the Reynolds-averaged equations for flows having a single length and time scale, the gradient-diffusion form is required by dimensional analysis but the model cannot handle multiple scales (Tennekes & Lumley 1972). The eddy-viscosity model of the SGS stress tensor is

$$\tau_{ij} = Q_{ij} - \tfrac{1}{3} Q_{kk}\, \delta_{ij} \sim -2\nu_T S_{ij}, \tag{7}$$

where ν_T is the eddy viscosity, and $S_{ij} = \frac{1}{2}(\partial \bar{u}_i/\partial x_j + \partial \bar{u}_j/\partial x_i)$ is the strain-rate tensor of the resolved scales; the SGS energy $\frac{1}{3}Q_{kk}$ can be combined with the pressure and has no dynamic effect.

Smagorinsky (1963) proposes an eddy-viscosity coefficient proportional to the local large-scale velocity gradient:

$$\nu_T = (C_S \Delta)^2 |S|. \tag{8}$$

Here, C_S is a constant, the filter width Δ is the characteristic length scale of the smallest resolved eddies, and $|S| = \sqrt{S_{ij} S_{ij}}$. This model and its variants have been used in numerical simulations with considerable success. Assuming that scales of $O(\Delta)$ are within an inertial subrange so that $|S|$ can be found from Kolmogorov's spectrum, the analysis of Lilly (1966), with a Kolmogorov constant of 1.5, gives values of C_S from 0.17 to 0.21, depending on the numerical approximation for S_{ij}. Subsequent investigators determine C_S in an empirical manner. In large-eddy simulations of decaying isotropic turbulence, Kwak et al. (1975), Shaanan et al. (1975), Ferziger et al. (1977), and Antonopoulos-Domis (1981) obtain C_S by matching the computed energy-decay rate to the experimental data of

Comte-Bellot & Corrsin (1971). For several computational grid volumes and different filters they find C_S to be in the range 0.19–0.24. None of these calculations extends to an inertial subrange, and different treatments of the Leonard stresses and numerical methods are used; thus, the small variation of C_S indicates its insensitivity to the details of the energy-transfer mechanism in isotropic turbulence.

In a simulation of high-Reynolds-number turbulent channel flow, Deardorff (1970) finds that the use of the value of C_S estimated by Lilly causes excessive damping of SGS intensities, but that a value of 0.1 gives energy levels close to those measured by Laufer (1951). Deardorff (1971) attributes this difference in C_S to the presence of mean shear, which is not accounted for in Lilly's analysis. In the calculation of inhomogeneous flows without mean shear, where buoyancy is the primary driving mechanism, Deardorff (1971) finds $C_S = 0.21$ appropriate. Lower values lead to excessive accumulation of energy in one-dimensional energy spectra near the cutoff wave number.

Using flow fields generated by direct numerical simulation of decaying isotropic turbulence at low Reynolds number, Clark et al. (1977, 1979) and McMillan & Ferziger (1979) tested the accuracy of Smagorinsky's model and calculated C_S. They give values of C_S comparable to those obtained empirically in the large-eddy simulations. McMillan et al. (1980), using data from direct simulations of strained homogeneous turbulence, find that C_S decreases with increasing strain rate, which confirms the conclusions of Deardorff (1971). With the mean strain rate removed from the computation of the model, C_S is nearly independent of the mean strain, a highly desirable property for the model. Fox & Lilly (1972) point out that the removal of the mean shear might have allowed Deardorff (1970) to use the higher C_S value of Lilly.

In addition to calculating model parameters, direct simulations are also used to determine how well the forms of the SGS models represent "exact" SGS stresses. For isotropic turbulence, the results show that the stresses predicted by Smagorinsky's model (and other eddy-viscosity models) are poorly correlated with the exact stresses. The model performance is worse still in homogeneous flows with mean strain or shear. The notable success of calculations using the Smagorinsky model seems to reflect the ability of this model to stabilize the calculations, and also shows that low-order statistics of the large scales are rather insensitive, in the flows considered, to the details of the SGS motions.

Several alterations and extensions to Smagorinsky's model have been proposed. A modification consistent with the classical two-point closures replaces the local magnitude of the strain-rate tensor, $|S|$, in (8) with its ensemble average $\langle S \rangle$ (Leslie & Quarini 1979). Although in numerical

solutions of the Burgers equation (Love & Leslie 1979) this modification improves the results, direct testing in isotropic flow by McMillan & Ferziger (1979) shows only a slight improvement. For free-shear flows, Kwak et al. (1975) suggest that it is appropriate to use the magnitude of vorticity $|\omega|$, rather than $|S|$, in (8), because the former vanishes in an irrotational flow. For isotropic turbulence this modification does not cause significant differences in large-scale statistics, but a substantial disparity is reported in small-scale statistics such as the velocity derivative flatness (Ferziger et al. 1977), which indicates the sensitivity of the smallest resolved scales to the SGS model. To account for mean shear in an LES of turbulent channel flow, Schumann (1975) introduces a two-part eddy-viscosity model. One part models the SGS stress fluctuations, and the other part, which reduces to Prandtl's mixing-length model for very coarse grids, accounts explicitly for the contribution of the mean shear.

When the grid resolution near a solid boundary is inadequate, the SGS flow field includes highly dynamic anisotropic eddies that contribute a significant portion of the total turbulence production and do not take a passive and dissipative role. Moin & Kim (1982), like Schumann, use a two-part eddy-viscosity model to account fully for the contributions to energy production by the finely spaced high- and low-speed streaks near the wall (see Section 4 and Kline et al. 1967) that are not adequately resolved in the spanwise direction:

$$\tau_{ij} = -\nu_T(S_{ij} - \langle S_{ij}\rangle) - \nu_T^*(y)\langle S_{ij}\rangle. \tag{9}$$

Here $\langle\ \rangle$ indicates an average over planes parallel to the walls. The first term in (9), the Smagorinsky model with mean shear removed, has essentially dissipative and diffusive effects on the resolvable scale turbulence intensities, $\sqrt{\langle(\bar{u}_i - \langle\bar{u}_i\rangle)^2\rangle}$. The second term accounts for the SGS energy production corresponding to SGS dissipation of mean kinetic energy $\langle\bar{u}\rangle^2$ but, in contrast to the first term, does not contribute to the dissipation of resolvable-scale turbulent kinetic energy. It does, however, indirectly enhance resolvable-scale energy production by representing the effect of the SGS stresses on the mean-velocity profile. Indeed, when Moin & Kim (1982) excluded the second term of (9) the computed flow did not transfer sufficient mean energy to the turbulence to sustain it against *molecular* dissipation. The characteristic length scale associated with ν_T^* is Δ_3, the filter width in the spanwise direction (normal to the mean flow and parallel to the wall), multiplied by an appropriate wall-damping factor to account for the expected y^3 or y^4 behavior of the Reynolds shear stress near the wall ($y = 0$). The influence of ν_T^* diminishes as the resolution of the spanwise direction is increased and the wall-layer streaks are better resolved.

Eddy-viscosity models of the type described above implicitly assume that

the SGS turbulence is in equilibrium with the large eddies and adjusts itself instantaneously to changes of the large-scale velocity gradients. It may be desirable (certainly in transitional flows) to allow a response time for the SGS eddies to adjust to the changes in the resolvable flow field. Following Prandtl, Lilly (1966) assumes an eddy viscosity proportional to the SGS kinetic energy q^2, i.e. $\nu_T = c\Delta q$. The equation for q^2, derived formally from the Navier-Stokes equations, contains several terms that must be modeled. Schumann (1975) successfully uses this model for the fluctuating SGS stresses in his calculation of turbulent flows in channels and annuli. Grotzbach & Schumann (1979) extend the model to lower Reynolds numbers. In addition to dividing the SGS stresses into mean and fluctuating parts, a noteworthy feature of Schumann's formulation is its explicit allowance for anisotropic grids. Different characteristic length scales and dimensionless coefficients determined by grid geometry appear in the representation of the various surface-averaged SGS stresses. The utility of the model is demonstrated by its ability to simulate turbulent flow in an annulus, with relatively high grid anisotropy, by changing only the mesh-geometry parameters. Parameters of a physical nature retained the values used in the channel flow calculations (Schumann 1975).

Deardorff (see Fox & Deardorff 1972) finds that the Smagorinsky model smears out the mean temperature gradient that occurs when buoyant convection is terminated by a stably stratified overlayer. For a more realistic model, Deardorff (1973) resorts to transport equations for the SGS stresses. This involves 10 additional partial differential equations. The closure models in these equations are essentially analogous to the corresponding models in the Reynolds-averaged equations. These models may not be appropriate because the behavior and relative importance of the various correlations involving only small scales are different than those involving the total turbulence (Ferziger 1982). Although the transport model does lead to improved results, the prospect of such a complex treatment of the SGS stresses is less attractive to us than a judicious distribution of mesh points and the possibility of extracting more-accurate models directly from information carried at the resolved scales.

In the discussion of the equations and models for LES we have considered flows in which the statistics of interest are determined by the large scales. This is appropriate for engineering purposes, but there are also very fundamental and interesting questions about the small scales to be answered. These are concerned with intermittency and structure at small scale, and the implications for Kolmogorov's universal equilibrium hypothesis and its later modifications. Siggia (1981) outlines a conceptual procedure analogous to LES in which the large scales are modeled and the small scales are computed. The model for the missing large scales appears as

a forcing term in the equations for the small scales. Siggia argues that if the large-scale effects depend on a small number of parameters (the dissipation rate is an obvious one) and the model is accurate enough, the limited scale range of the simulation might represent the intermittency achieved by the larger range of scales occurring at high Reynolds numbers. Unfortunately this is not possible in a calculation based on a periodic field in a fixed mesh, because the small-scale spatial intermittency that can be represented is directly limited by the number of mesh points and this geometric constraint cannot be modeled away. The vortex method of Leonard (1980) is not grid limited and is a more natural way to describe the intermittent vorticity fields occurring at high Reynolds numbers.

4. RESOLUTION REQUIREMENTS

Over two decades ago Corrsin (1961) demonstrated that the direct numerical simulation of high-Reynolds-number flows places an overwhelming demand on computer memory and speed. [See Chapman (1979) for a comprehensive study of the grid requirements for computational aerodynamics.] In direct simulations the number of spatial grid points is determined by two constraints: first, the size of the computational domain must be large enough to accommodate the largest turbulence scales (or the scale of the apparatus), and second, the grid spacing must be sufficiently fine to resolve the dissipation length scale, which is on the order of the Kolmogorov scale, $\eta = (\nu^3/\varepsilon)^{1/4}$. The ratio of these two scales (cubed) provides an estimate for the total number, N, of mesh points. In turbulent channel flow, for example, macroscales in the directions parallel to the walls determined from the two-point correlation measurements of Comte-Bellot (1963) and the average dissipation rate $\varepsilon = u_\tau^2 U_m/\delta$ give $N \simeq (6\mathrm{Re}_m)^{9/4}$ (Moin 1982); here Re_m is the Reynolds number based on the channel half-width, δ, and the average flow speed, U_m; and $u_\tau = \sqrt{\tau_w/\rho}$ is the wall shear velocity determined by the shear stress at the wall, τ_w, and the fluid density ρ. It is assumed that four grid points in each direction are required to resolve an eddy, and that $U_m/u_\tau \simeq 20$. Temporal resolution of the smallest computed eddies requires the time step Δt to be on the order of $(\nu/\varepsilon)^{1/2} = (\delta/u_\tau)\,\mathrm{Re}_m^{-1/2}$. At the moderate Reynolds number $\mathrm{Re}_m = 10^4$, roughly 5×10^{10} grid points and 2×10^3 time steps are necessary for the flow to reach a statistically steady state (a total flow time of $100\delta/U_m$). Such a computation is beyond the capabilities of presently available computers. However, if the bulk of the dissipation occurs at scales larger than 10η rather than η, direct simulation of channel or pipe flow may be possible in the near future at the lowest Reynolds numbers studied experimentally ($\mathrm{Re}_m \sim 2500$; see Eckelmann 1974).

In contrast to wall-bounded turbulent shear flows, which cannot be sustained below a critical Reynolds number, homogeneous and free-shear flows remain turbulent at Reynolds numbers for which all scales of motion can be resolved. The large-scale features of these flows are nearly independent of Reynolds number, and statistics determined from them are relevant at higher Reynolds numbers. However, in the simulation of unbounded shear flows such as turbulent jets and mixing layers (especially at low Reynolds numbers), the computational domain must be large enough to allow development of the long wavelength instability typical of these flows.

In LES the resolution requirements are determined directly by the range of scales contributing to the desired statistics and indirectly by the accuracy of the model. The less accurate the model, the further the modeled scales must be separated from the scales of interest. In engineering calculations the important scales contain the dynamic physical events responsible for turbulent transport of heat and matter and the production of turbulent energy. Near walls the principal flow structures are high- and low-speed streaks, which are finely spaced in the spanwise direction (Kline et al. 1967) and provide most of the turbulence energy production. The mean spanwise spacing of the streaks is about 100 wall units ($100\nu/u_\tau$), but streaks as narrow as 20 wall units probably occur and would require $h_3^+ \sim 5$ for complete spanwise resolution (Moin 1982). Similar considerations in the streamwise direction lead to $h_1^+ = 20$ to 30. Using 64 grid points normal to the wall (with nonuniform spacing to resolve the viscous sublayer and outer layers) and with computational periods in directions parallel to the walls chosen in accordance with two-point correlation measurements, the total number of grid points is estimated to be $N \sim 0.06\ \mathrm{Re}_m^2$. Although at high Reynolds numbers this is prohibitively large, detailed simulation of the important large eddies can be performed at low Reynolds numbers ($\mathrm{Re}_m \sim 5000$) with presently available computers. The Reynolds number of resolvable flows can be significantly increased when a fine mesh in the lateral directions is embedded near the walls (Chapman 1979), but for practical applications much computer power is still needed to calculate the flow in this extremely thin layer. If the wall-layer dynamics can be replaced by reliable outer-flow boundary conditions (see Section 5.2), the number of grid points becomes low enough to use LES for engineering computations on current computers (Chapman 1981).

Another practical difficulty in both direct and large-eddy simulations is the cost of obtaining an adequate sample for the flow statistics. The various scales of motion are not equally sampled; the scale sample is inversely proportional to the scale volume. With appeal to the ergodic hypothesis, ensemble averages can be replaced by averages over homogeneous space-

time dimensions. For low-order velocity statistics a sample of 10^3 nodes appears adequate, but much larger samples are required for statistics of intermittent velocity derivatives and this problem increases with Reynolds number (Fox & Lilly 1972, Ferziger et al. 1977, Siggia 1981). When the homogeneous dimensions (there is usually at least one) do not provide an adequate sample, the statistics can be collected from an ensemble of flows evolving from independent initial conditions, but this is very costly and poses a serious problem for simulation of inhomogeneous flows.

5. NUMERICAL METHODS

Numerical implementation of the governing equations consists of four main issues: numerical approximation of spatial derivatives, initial and boundary conditions, time-advancement algorithm, and computer implementation and organization. In each category there are options available, and the choice of the overall algorithm depends on the problem under consideration, the cost, and the computer architecture.

5.1 *Spatial Representation*

Second- and fourth-order finite differences and spectral methods are used to approximate spatial derivatives. Since turbulent flows involve strong interaction among various scales of motion, special care should be taken that numerical representation of derivatives be faithful to the governing equations and the underlying physical mechanisms. For example, approximations with appreciable artificial viscosity, such as upwind difference schemes, significantly lower the effective Reynolds number of the calculation, and their dissipative mechanism distorts the physical representation and dynamics of large as well as small eddies. The formal order of accuracy associated with a difference method, which defines the asymptotic error for infinite resolution, may be less important than the accuracy of the method at the coarse resolution applied at the smallest computed scales. The accuracy of a method at various scales is illustrated by its ability to approximate the derivative of a single Fourier mode e^{ikx} (Mansour et al. 1979). For a given number of grid points, all difference schemes are inaccurate for values of wave number k near π/h, the highest wave number that can be represented on the grid. However, for intermediate values of k some schemes are significantly more accurate than others having the same formal order of accuracy.

The spectral method (Gottlieb & Orszag 1977) is a very accurate numerical differentiator at high k values. In this method the flow variables are represented by a weighted sum of eigenfunctions, with weights determined using the orthogonality properties of the eigenfunctions. The

derivatives are obtained from term-by-term differentiation of the series or by using the appropriate recursion relationships (Fox & Parker 1968). The choice of eigenfunctions depends on the problem and the boundary geometry and conditions. For problems with periodic boundary conditions Fourier series are the natural choice, but for arbitrary boundary conditions orthogonal polynomials that are related to the eigenfunctions of singular Sturm-Liouville problems should be used (Gottlieb & Orszag 1977). Expansions based on these polynomials do not impose parasitic boundary conditions on higher derivatives, and for smooth functions they provide rapid convergence independent of the boundary conditions.

The difference between spectral and "pseudo-spectral" approximations is in the way products are computed (Orszag 1972). The advantage of the more expensive spectral method is the exact removal of aliasing errors (Orszag 1972); Patterson & Orszag (1971) give efficient techniques for handling aliasing errors arising in bilinear products. These errors are not peculiar to pseudo-spectral methods; finite-difference approximations of products also contain aliasing errors, but the errors are less severe owing to the damping at high k of the difference approximations. Aliasing errors usually increase with the order of accuracy of difference schemes (Orszag 1971).

One serious consequence of aliasing errors is the violation of the invariance properties of the Navier-Stokes equations. It is easily shown that in the absence of viscous terms and time-differencing errors, the governing equations conserve mass, momentum, energy, and circulation. Aliasing errors can violate these invariance properties and lead to nonlinear numerical instabilities (Phillips 1959). Lilly (1964) demonstrates that the staggered-mesh difference scheme (see Harlow & Welch 1965) preserves these invariance properties. When the nonlinear terms in the momentum equations are cast in the rotational form, $\boldsymbol{\omega} \times \mathbf{u} + \nabla(\mathbf{u}^2/2)$, properly invariant numerical solutions are obtained with pseudo-spectral and most finite-difference methods (Mansour et al. 1979).

For sufficiently smooth functions, spectral methods are more accurate than difference schemes having the same number of nodes. In contrast to higher-order difference methods, which require special treatment near the boundaries, spectral methods allow proper imposition of the boundary conditions. However, for the flow field to be sufficiently smooth, the smallest scale of motion present should be well resolved on the computational grid; otherwise, the rapid convergence of spectral methods is badly degraded. Cost constraints usually prohibit thorough resolution of the small scales; in direct simulations this means a mesh too coarse to capture the dissipation scales and in LES calculations means a filter or SGS model that does not remove sufficient energy from the small scales. In simulations

of "two-dimensional turbulence" in a periodic box, Herring et al. (1974) find that the accuracy of spectral calculations is comparable to that of second-order (conservative but aliased) difference calculations having approximately twice the number of grid points in each direction. The advantage of the spectral method as an accurate differcntiator is limited by the error that arises from truncation of small scales produced by the nonlinear terms.

A very important attribute of spectral methods is their self-diagnosis property. Inadequate grid resolution is reflected in excessive values of high-order expansion coefficients (Herring et al. 1974, Moin 1982). Fourier analysis of finite-difference solutions can also reveal poor resolution (Grotzbach 1981), but damping at high wave numbers masks its detection until the computational grid is insufficient to represent even the larger scales of motion.

5.2 *Boundary and Initial Conditions*

In turbulence simulations, the major difficulty with specification of boundary conditions occurs at open boundaries where the flow is turbulent. The flow variables at these boundaries depend on the unknown flow outside the domain. The unavoidably ad hoc conditions specified at these boundaries should be designed to minimize the propagation of boundary errors. Periodic boundary conditions are generally used for directions in which the flow is statistically homogeneous, but this implies that quantities at opposite faces of the computational box are perfectly correlated. If the periodic solution obtained is to represent turbulence, thc period must bc significantly greater than the separation at which two-point correlations vanish. The computed two-point correlation functions then serve as a good check of the adequacy of the size of the period.

Periodic boundary conditions for homogeneous turbulence subjected to uniform deformation may be applied only in a coordinate system moving with the (linear) mean flow. In this system the mean convection relative to the mesh vanishes, and the equations do not refer explicitly to the space variables. However, the computational grid is being continuously deformed, and the calculations must be stopped when the domain becomes so distorted that the flow cannot be resolved in all directions (Roy 1982). In the case of uniform shear, a convenient remeshing procedure (Rogallo 1981, Shirani et al. 1981) allows the computations to continue until the scale of the largest resolved eddies becomes bounded by the period. A clever implementation of the procedure for a finite-difference calculation by Baron (1982) uses shifting boundary values on a fixed mesh. The problem of length-scale growth is common to both experiments and computations. In homogeneous flows or unbounded inhomogeneous flows, the macroscales of turbulence grow until they reach the dimensions of the wind tunnel or the

size of the computational box. When this occurs, meaningful statistics cannot be obtained from the large scales. To study the evolution of the flow for longer times it is tempting to use a coordinate transformation that continuously expands the computational box in time, but such a transformation reintroduces explicit spatial dependence in the governing equations. On the other hand, the calculation can be interrupted and the mesh rescaled to cover a new range of larger scales. The interpolation of the existing field to the new mesh causes some information loss; to minimize the damage the process should be carried out while the two-point correlations still show a significant uncorrelated range.

One of the more challenging, and virtually untouched, problems is that of turbulent inflow and outflow boundary conditions in nonhomogeneous directions. The inflow problem appears to be more troublesome, since in most cases the influence of the upstream conditions persists for large distances downstream. Of course, one way to avoid the problem is to prescribe a small orderly perturbation on an incoming laminar flow and follow the flow through transition to turbulence. However, in addition to more stringent requirements on the treatment of the small-scale motions in transitional flows, the required length of the computational box for the entire process is prohibitively large in some cases. The use of turbulent inflow and outflow conditions appears to be a practical necessity for flows such as boundary layers, where linear-stability theory predicts a long transitional zone.

The implementation of inflow and outflow conditions in simulations of free turbulent shear flows has so far been avoided by use of the "frozen turbulence" approximation. The physical problem, which is homogeneous in time but not in the mean-flow direction, is replaced by a computational problem that is homogeneous in the flow direction but not in time. The inflow condition is replaced by an initial condition, and periodic boundary conditions in the mean-flow direction are applied. Although the time-developing approximation of the "real flow" has most of its features, important differences remain. In a spatially developing turbulent mixing layer, for example, the mean streamlines within the layer are inclined to the direction of the flow outside the layer, but those in the time-developing flow are not.

Two approaches have been taken for implementing irrotational free-stream conditions in free-shear flows. Orszag & Pao (1974), Mansour et al. (1978), and Riley & Metcalfe (1980a) use a finite computational domain with stress-free boundary conditions in which the normal velocity and the normal derivative of the tangential velocities are zero. The turbulence field is confined to the central region of the domain and is surrounded by irrotational flow that extends to the boundaries. The subsequent use of

Fourier series implies the existence of image flows above and below the computational box that influence the dynamics of the flow inside. A better approach (Cain et al. 1981) maps the infinite domain into a finite computational box and applies the free-stream (or no-stress) boundary conditions at the boundaries of the transformed domain. The coordinate transformation used by Cain et al. allows a fairly simple use of Fourier spectral methods.

The specification of boundary conditions at smooth solid boundaries does not pose any difficulty; the velocity at the wall is the wall velocity. In the vicinity of the wall, the flow field is composed of small, energetic eddies associated with large mean-velocity gradients (see Section 4). For practical applications it is desirable to avoid the high cost of resolving this wall region by replacing flow near the wall with boundary conditions applied somewhat away from the wall. In simulations of high-Reynolds-number turbulent channel flow, Deardorff (1970) and later Schumann (1975) modeled the flow near the wall by applying such boundary conditions in the logarithmic layer. Once again it is not clear how to specify boundary conditions within a turbulent flow. For example, Schumann (1975) assumes that the fluctuations of wall shear stress, τ_w, are perfectly correlated with those of the streamwise velocity one mesh cell from the wall. Space-time correlation and joint probability density measurements of τ_w and u by Rajagopalan & Antonia (1979) support this assumption very close to the wall provided that a (sizable) time delay between these two quantities is introduced (see also Eckelmann 1974). The accuracy of this assumption degrades as the point of application of boundary conditions moves away from the wall; the normalized correlation is unity at the wall but is only about 0.5 in the logarithmic layer at $y^+ = 40\,(y/\delta = 0.031)$ (Rajagopalan & Antonia 1979). However, Robinson (1982) reports a correlation as high as 0.7 at $y^+ = 300\,(y/\delta = 0.03)$ in experiments at an order of magnitude higher Reynolds number ($Re_\theta = 32{,}800$). These experimental results indicate that the u-τ_w correlation at a fixed y^+ improves with increasing Reynolds number, but at least part of this apparent improvement results from inadequate probe resolution at high Reynolds numbers. Robinson's wire length extends 200 wall units in the spanwise direction. Nevertheless, Schumann's assumption of u-τ_w correlation is reasonable and can be improved by including a space-time shift. Chapman & Kuhn (1981) propose a two-dimensional wall-layer structure retaining only the transverse spatial variation. They use detailed experimental data to set the length scales and phase relations of the velocity at the outer edge of the layer and obtain good agreement with experiment for the internal layer structure. Their wall-layer edge conditions have not yet been used as boundary conditions for the outer flow. The detailed pressure-velocity data provided

by simulation (Moin & Kim 1982, Kim 1983) should be useful for the formulation of wall-layer edge conditions of the kind proposed by Chapman & Kuhn.

A three-dimensional velocity field satisfying the continuity equation and boundary conditions must be specified to initialize the calculation. Within these constraints, a random fluctuating velocity field is superimposed on a prescribed mean-velocity profile. Although the initial turbulence field can be defined with the desired intensity profiles and energy spectra, its higher-order statistics become physically realistic only after an adjustment period (see Orszag & Patterson 1972, Riley & Metcalfe 1980a). For example, the velocity derivative skewness is initially zero but quickly rises to a realistic value. The evolution of time-developing flows (those that never reach a statistically steady state) is often quite sensitive to the initial conditions for the large scales.

5.3 *Time Advancement*

Starting from initial conditions, the governing equations are advanced in time subject to the incompressibility constraint. We discuss time-advancing algorithms as they are applied to the incompressible Navier-Stokes equations. The additional SGS terms in the LES equations pose little additional numerical difficulty, and virtually identical numerical methods are used.

Time advancement may be done either explicitly or implicitly; explicit schemes are much easier to implement and have a much lower cost per step. The popular second-order explicit Adams Bashforth and Leapfrog schemes require only one evaluation of the time derivatives per step, but they do require retention of variables at step $n-1$ in order to advance from step n to $n+1$. The self-starting Runge-Kutta schemes (second, third, and fourth order) cost more per step but have better stability properties and therefore allow larger steps. The multiple evaluations of nonlinear terms required by Runge-Kutta methods can be used to reduce the cost of controlling aliasing errors in Fourier spectral calculations (Rogallo 1981).

When using explicit methods, the incompressibility constraint at each time step is usually enforced by solving a Poisson equation for pressure rather than by direct use of the continuity equation. To satisfy the discrete continuity constraint, the discrete Poisson problem must be derived using the same differencing operators used in the discrete momentum and continuity equations (Kwak et al. 1975). The staggered-grid difference scheme (see Harlow & Welch 1965) leads to a particularly simple Laplacian operator, whereas with standard centered-difference methods the operator is less compact and causes spatial pressure oscillations due to the uncoupling of even and odd points.

The choice of proper boundary conditions for the pressure equation is ambiguous (Moin & Kim 1980). Usually the Neumann boundary condition obtained from the normal momentum equation is used, but a Dirichlet boundary condition can also be derived from the tangential momentum equations. When spectral methods are used with explicit time advancement, the fact that both conditions cannot be simultaneously enforced implies the inability to impose complete velocity boundary conditions (Moin & Kim 1980). With the second-order staggered finite-difference scheme, the need for pressure boundary conditions does not arise. The continuity equation at the interior cells, together with the momentum equations (at the interior grid points) and the velocity boundary conditions, leads to a closed system of algebraic equations for pressure.

The root of this difficulty with spectral methods is that explicit methods treat the governing equations as an initial-value problem rather than as a boundary-value problem. Implicit methods require the solution of a boundary-value problem at each time step, thus allowing the natural imposition of velocity boundary conditions. Moreover, in simulations of wall-bounded flows, implicit treatment of the viscous terms overcomes the severe restriction on time step that arises from the small grid spacing normal to the wall. For these reasons all the calculations that extend to the wall use semi-implicit time-advancement algorithms (Orszag & Kells 1980, Moin & Kim 1980, 1982, Kleiser & Schumann 1979). In these calculations the nonlinear terms are advanced by the Adams Bashforth method. Fourier expansions are used in homogeneous dimensions, and either Chebyshev polynomial expansions or second-order difference methods are used in the direction normal to the wall. Recently, Leonard & Wray (1982) have developed a semi-implicit spectral method based on expansion in divergence-free vector functions. In this representation of the velocity, each term satisfies the continuity equation as well as the boundary conditions. Since the continuity constraint is satisfied by the expansion functions, pressure does not appear and only two velocity components are required to define the velocity field; this significantly reduces computer memory requirements. In wall-bounded flows the time step required for accurate resolution (see Section 4) is much larger than that required for convective stability, which suggests that advancement of the convective terms by implicit methods may be advantageous. Deardorff (1970) and Schumann (1975) translate the coordinate system at constant speed, reducing the mean convection velocity relative to the mesh to allow increased time steps. Alternatively, convection by the mean velocity can be handled implicitly; this is much simpler than a complete implicit treatment.

For problems in general geometries the computational complexity of spectral algorithms is not appreciably greater than that of difference

algorithms when the boundary conditions allow use of explicit time advancement and the physical domain can be analytically mapped to a simple computational domain. But the linear convective stability criterion for the explicit advancement is more severe (by a factor of π for second-order central differences). With fully or partially implicit time advancement the computational complexity of spectral algorithms is much greater than that of difference algorithms. The nonconstant coefficients that arise when a complicated physical domain is mapped to a simple computational domain lead to dense matrix equations for the spectral coefficients. It is impractical to solve these equations by direct techniques; only iterative procedures appear to be feasible (Orszag 1980), and the accuracy and efficiency of the method depend on the number of iterations required to obtain the converged solution at the next step.

6. RESULTS

The flows simulated to date fall into one of three classes: homogeneous (unbounded), unbounded inhomogeneous, and wall bounded. The emphasis of the work can be classified as fundamental physics, development of simulation technique, and application to real problems. In the preceding sections we have discussed some of the work on technique. In this section we present typical fundamental results for three simple shear flows: homogeneous turbulence in uniform shear, the evolution of a turbulent mixing layer, and turbulent channel flow. These flows exhibit many of the complications found in real engineering problems. The homogeneous shear flow introduces anisotropy and production at large scales, the mixing layer adds turbulent diffusion and intermittence at the large scales, and the channel introduces solid boundaries near which all of these complications occur at small scales as well. These three flows are well documented by high-quality experimental data and have been simulated using a variety of numerical methods and a range of resolution.

Turbulence in uniform shear exhibits growing length scales, $O(L)$, and velocity scales, $O(q)$, which appear to approach fixed ratios as the flow evolves (Harris et al. 1977), and the characteristic time of the turbulence, $O(L/q)$, locks on to the characteristic time of the shear, $O(S^{-1})$. It is plausible that the turbulence ultimately attains a self-similar structure with exponential growth of length and velocity scales (Rogallo 1981). The early evolution of isotropic turbulence subjected to uniform shear is predicted well by the linear theory of rapid distortion (Deissler 1961, 1972). Although this theory incorrectly predicts ultimate turbulence decay, its prediction of the Reynolds-stress anisotropy and two-point correlations is surprisingly accurate (Townsend 1976). The first simulation of homogeneous shear was

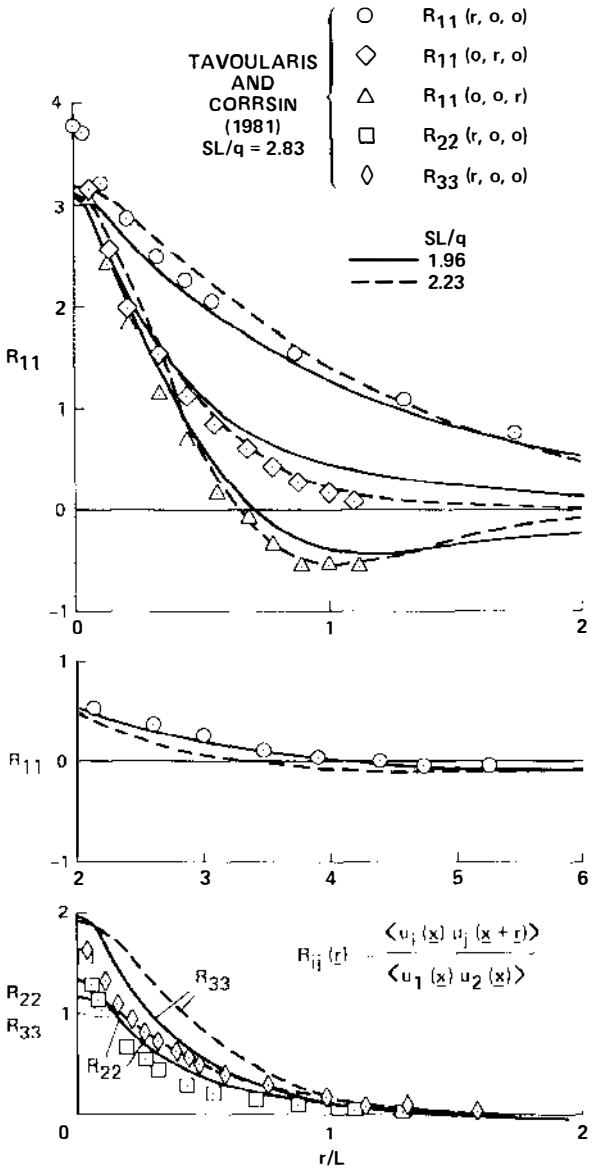

Figure 1 Self-similarity of the autocorrelations in homogeneous shear turbulence (from Rogallo 1981).

the 16 × 16 × 16 finite-difference LES by Shaanan et al. (1975). Their results agree qualitatively with the experimental data, even though periodic boundary conditions were applied on a fixed mesh (see Section 5). More details of the flow are obtained in the 64 × 64 × 64 direct spectral simulations of Feiereisen et al. (1981) and Shirani et al. (1981) in which compressibility effects and passive scalar transport, respectively, are studied. The results of Rogallo's (1981) 128 × 128 × 128 direct spectral simulation indicate that even at a macroscale Reynolds number an order of magnitude below that of Tavoularis & Corrsin (1981), the large-scale statistics of the experiment can be reproduced. A major difficulty is the definition of a characteristic length for the energy-containing scales. The integral scale depends strongly on the largest computed scales for which the statistical sample is poor. In Figure 1 the computed correlations for two simulations are compared with the data of Tavoularis & Corrsin. The correlations are normalized by the turbulent shear stress rather than normal stresses, and the separation is made nondimensional by reference to the longitudinal integral scale in the mean-flow direction. This scaling should collapse the correlations of the large scales; the correlations of streamwise velocity collapse well for the different Reynolds numbers and characteristic times ratios, SL/q, but collapse for the transverse velocity components is less satisfying.

The calculated flow fields can be used as detailed data for the development and testing of closure models. As an example, the tensor sum of the pressure-strain correlation (the "slow" term) and the deviator of dissipation,

$$\varepsilon\phi_{ij} = -2pS_{ij} + 2(\varepsilon_{ij} - \tfrac{1}{3}\varepsilon\delta_{ij}), \qquad \varepsilon_{ij} = \nu \overline{\frac{\partial u_i}{\partial x_k}\frac{\partial u_j}{\partial x_k}}, \quad \varepsilon = \varepsilon_{ii} \tag{10}$$

is usually modeled in a Reynolds-stress closure (Lumley 1980) by a scalar multiple of the Reynolds-stress anisotropy tensor, $\phi_{ij} \sim \beta b_{ij}$, where $b_{ij} = u_i u_j / u_k u_k - \frac{1}{3}\delta_{ij}$.

Lumley proposes that the scalar coefficient depends on Reynolds number, the invariants of the stress tensor, and other relevant scalars of the flow. The two tensors (Figure 2*a*) are indeed correlated in the calculated fields, and the collapse obtained by the linear model (Figure 2*b*) supports its use (but its performance in other anisotropic homogeneous flows does not;

Figure 2 Lumley's (1980) linear model of pressure-strain correlation and dissipation anisotropy. (*a*) Dependence of modeled tensor on Reynolds-stress anisotropy tensor; (*b*) comparison of modeled and measured values; (*c*) variation of model coefficient with Reynolds number. The data points represent independent flow fields at a wide range of parameters (from Rogallo 1981).

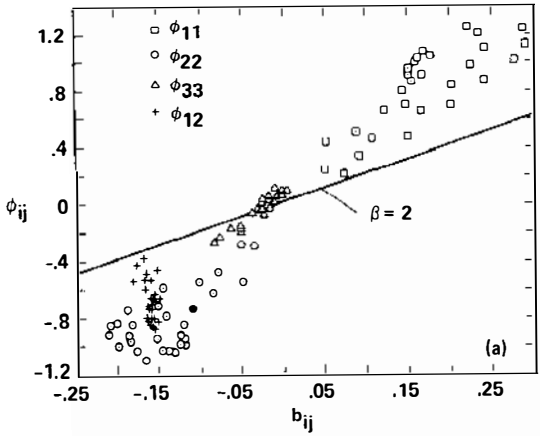

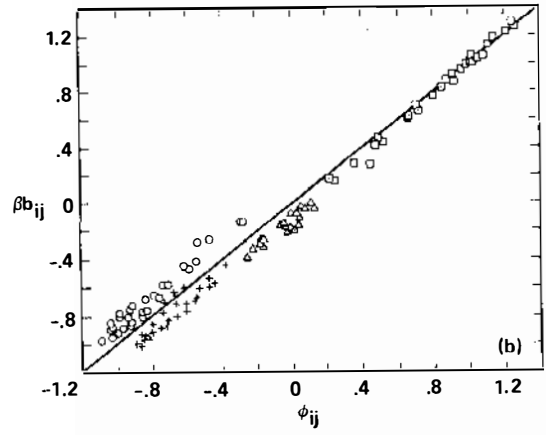

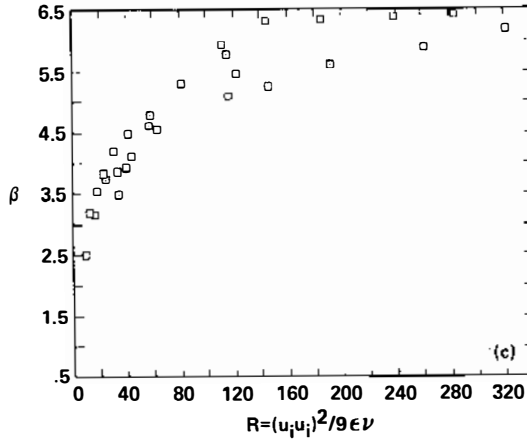

see Rogallo 1981). The orderly nature of the small remaining error suggests the possibility of higher-order model terms. The increase of the model coefficient, β, with Reynolds number (Figure 2*c*) has been predicted by Lumley, but it should be noted that other scalar attributes of the flow, particularly the ratio of shear and turbulence time scales, are important and they are also varying among the data shown.

The mixing layer separating two uniform streams of differing speed has been studied analytically, experimentally, and recently by simulation. Much of the recent work is concerned with the observed organized vortical structures that result from Kelvin-Helmholtz instability in turbulent layers and their downstream growth by pairing (Roshko 1976). It is found experimentally that the evolution of the layer is strongly influenced by imposed perturbations, and the simulations indicate an analogous sensitivity to initial conditions. Simulations of the LES type have been performed at low resolution by Mansour et al. (1978) and Cain et al. (1981). In the calculations of Mansour et al., the roll-up stage of the flow is inhibited by a mesh domain too short to support unstable waves. When vortex cores are included in the initial field the eddy-viscosity model, in the presence of the mean shear, prevents the proper growth of energy and length scales. The problem appears to be simply one of inadequate resolution. The mesh of Cain et al., on the other hand, is scaled to include the fundamental instability wave and its subharmonic. Roll up of the layer occurs, with the resulting vortices meandering in the spanwise direction and pairing locally to form a network of vortex tubes. Riley & Metcalfe (1980b), using a $32 \times 32 \times 32$ direct spectral simulation, show (as do Cain et al.) that the presence of an energetic two-dimensional instability wave modulates the layer growth; the early growth is more rapid, but once roll up has occurred growth is delayed until the vortices approach each other (by turbulent diffusion, convection by a subharmonic, spanwise variations in proximity, etc.) closely enough for pairing to occur. The spanwise vorticity field of a turbulent mixing layer (Figure 3*a*) clearly shows coherent structures, even though the layer growth is statistically self-similar. The structures are not simple two-dimensional vortices however, as the vorticity at another spanwise plane (Figure 3*b*) indicates. Metcalfe & Riley (1981) increase the computational domain to capture the subharmonic of the instability wave. These $64 \times 64 \times 64$ mesh results confirm their earlier results, and the larger domain eliminates a spurious growth of turbulence intensity found there. This flow illustrates the importance of not constraining potentially important scales, in this case the instability scale.

The most extensive application of LES has been the calculation of fully developed turbulent channel flow. In the first realistic numerical simulation

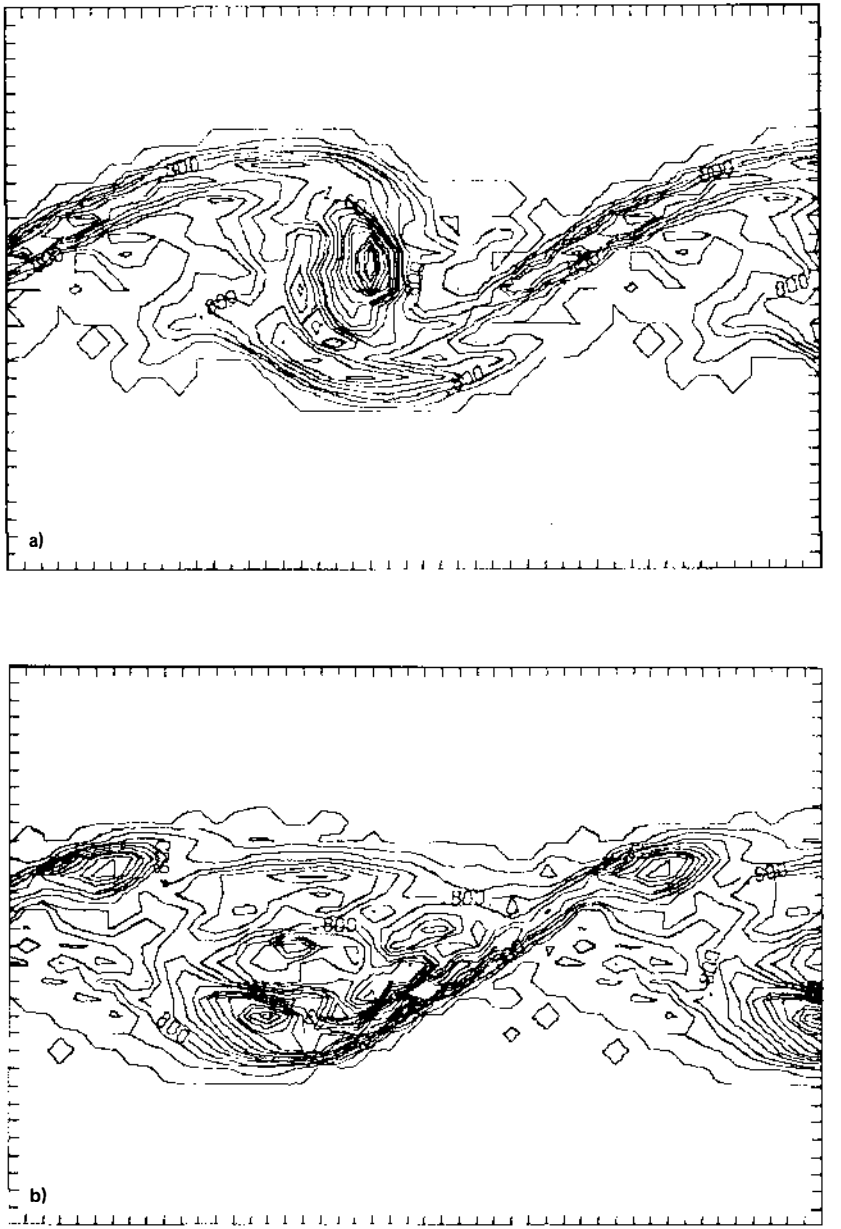

Figure 3 Distribution of the spanwise vorticity component in a turbulent mixing layer as viewed in the spanwise direction. The distribution is shown in two planes separated by half the computational period (from Riley & Metcalfe 1980b).

of turbulence, Deardorff (1970) calculated this flow at a very high Reynolds number using only 6720 grid points. Schumann (1975) and Grotzbach & Schumann (1979) used up to 65,536 grid points, included temperature fluctuations and heat transfer, and considered a range of moderate Reynolds numbers ($Re > 10^4$), but like Deardorff, they *modeled* the wall-layer dynamics. In these calculations the mean-velocity profile, turbulent intensities, and pressure statistics are in good agreement with the experimental data. Moin & Kim (1982) calculated the channel flow at $Re = 13{,}800$ (based on channel half-width δ and centerline velocity), and extended the calculations to the wall using a nonuniform mesh with total of 516,096 grid points. The computed velocity and pressure field was used to study the time-dependent structure of the flow and its relationship to

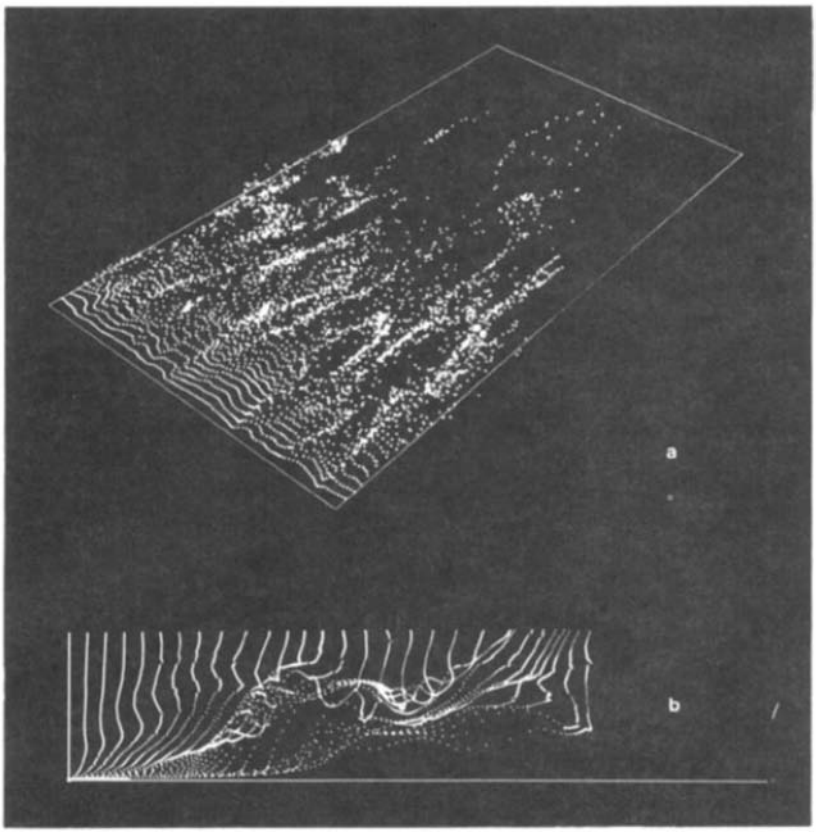

Figure 4 Turbulent channel flow visualized by fluid markers (simulated hydrogen bubbles). (*a*) Markers introduced on a line in the spanwise direction at $y^+ = 6$; (*b*) markers introduced on a line normal to the wall; view extends to $y^+ = 240$ (from data of Moin & Kim 1982).

various flow statistics (including those appearing in the time-averaged Reynolds-stress equations). The detailed flow field was analyzed with contour plots of the instantaneous velocity, pressure, and vorticity fluctuations; with higher-order statistical correlations; and with tracking of passive particles in the flow. In particular, a motion picture was made simulating hydrogen-bubble flow-visualization experiments (see Kim et al. 1971; Kline et al. 1967). In Figure 4 two typical frames from this film show the paths of bubbles generated near the wall ($y^+ \simeq 6$) along a line in the spanwise direction and of bubbles generated along a line normal to the channel wall. Various distinct flow features, including the wall-layer streaks (Figure 4*a*), and the formation of profiles with multiple inflection points and ejection of fluid from the wall region (Figure 4*b*), are in accordance with laboratory observations.

The contours of wall-pressure fluctuations from the turbulent channel flow simulations of Grotzbach & Schumann (1979) are shown in Figure 5. In agreement with experimental measurements (Bull 1967, Willmarth 1975), the large-scale pressure fluctuations are correlated at considerably greater distances in the lateral direction than they are in the mean-flow direction. This feature is reproduced in the calculations of Moin & Kim (1982), where localized regions of high pressure intensity are also observed. The two-point pressure correlations of Moin & Kim (1982) indicate that the spanwise elongation of pressure eddies persists across the entire channel. Figure 6 shows the two-point velocity and pressure correlations in the vicinity of the wall ($y/\delta = 0.06$, $y^+ = 38$). The pressure correlation is negative for large streamwise separations but is always positive for

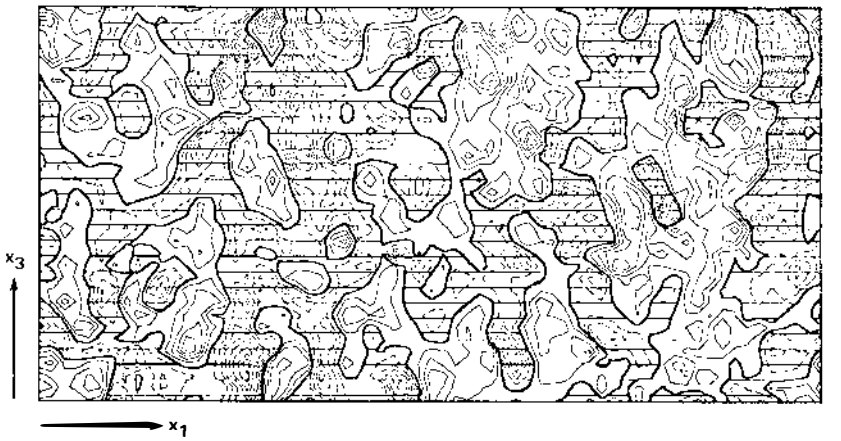

Figure 5 Pressure distribution at the wall in turbulent channel flow (from Grotzbach & Schumann 1979).

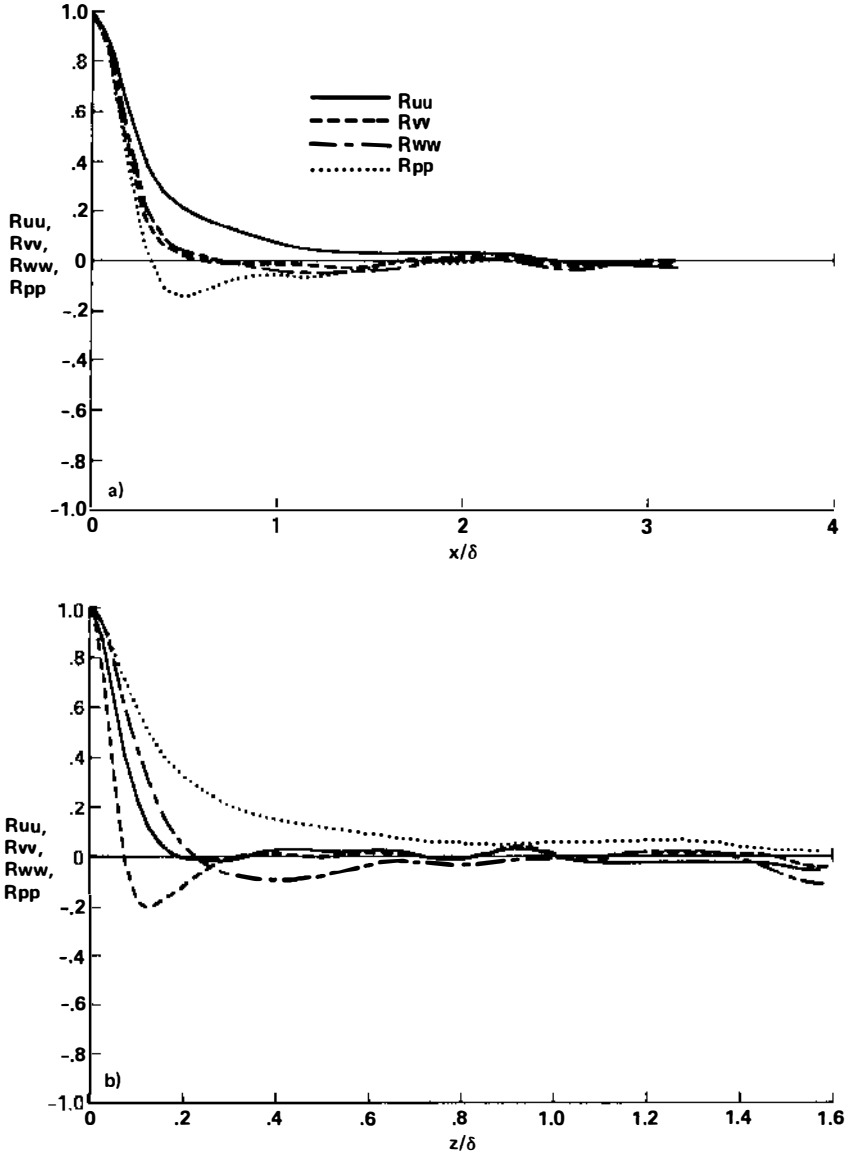

Figure 6 Two-point correlations of pressure and velocity near the wall ($y^+ = 38$) in turbulent channel flow. (*a*) Points separated in streamwise direction; (*b*) points separated in spanwise direction (from data of Moin & Kim 1982).

spanwise separations. The same characteristics are exhibited by experimentally measured wall pressure correlations (Bull 1967). Thus, the fluctuating pressure gradients driving the flow are stronger in the streamwise direction than in the spanwise direction. In the vicinity of the wall the pressure fluctuations are correlated over larger lateral distances than are the velocity components, but in the streamwise direction it is the velocity fluctuations (particularly the streamwise component) that are correlated over larger distances.

Recently, Kim (1983) has further studied the spatial structure of the wall layer by applying a conditional sampling technique to the "data" generated by Moin & Kim (1982). Figure 7 shows the signatures of the pressure and streamwise velocity component, during a "bursting event," obtained using a variant of the VITA conditional sampling technique of Blackwelder & Kaplan (1976). The velocity signatures are remarkably similar to the experimental results. The pressure signatures (which can be obtained experimentally only at the walls) indicate localized peaks during the detected bursting event, with adverse pressure gradient associated with flow deceleration. The pressure signature persists at significantly larger

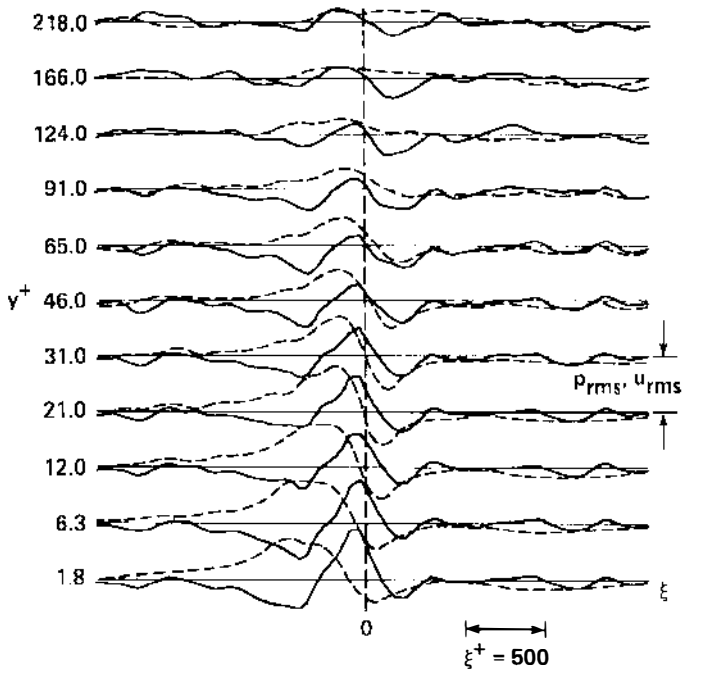

Figure 7 Pressure and velocity signatures of the "bursting event" near the wall in turbulent channel flow. ----- streamwise velocity; ——— pressure (from Kim 1983).

distances normal to the wall than does the velocity signature; this suggests that the fluctuating pressure gradient driving the wall layer is imposed by the outer flow. The conditionally averaged transverse velocity components and streamwise vorticity component, displayed in planes normal to the flow direction, show a distinct pair of counter-rotating vortical structures associated with the bursting process.

In addition to the fundamental studies outlined above, LES has also been used in practical engineering applications, where it can be more cost effective than the multiple transport equation statistical models (Schumann et al. 1980). For example, in a problem related to nuclear-reactor safety, Grotzbach (1979) used a very-coarse-grid ($16 \times 16 \times 8$) LES to investigate the effect of buoyancy on flow mixing in the downcomer of a reactor. He found that buoyancy enhances mixing of the entering hot and cold fluid streams and prevents a "hot chimney" from developing along the length of downcomer adjacent to the reactor core. These results were later confirmed by experimental measurements. LES appears to be the only viable predictive computational tool in applications that involve aerodynamic noise, reduction of turbulent skin friction (for example, flow over compliant boundaries), and other applications in which the details of turbulence dynamics play a dominant role.

7. SUMMARY

Numerical simulation has become a viable complement to experiment in both fundamental and applied turbulence research. Its growing popularity reflects both its promise of realistic answers to a difficult problem and the continuing rapid decline in computing costs. We expect this trend to continue. In addition to the advances in computer capacity of the last decade, less easily measured progress has been made in simulation technique and in the utilization of simulation results. A notable development in numerical algorithms has been the use of spectral methods for direct simulations in simple geometries. This method is not very attractive at present for complex LES calculations involving mesh mapping and implicit time advancement. The premise of LES, that turbulence calculations can be closed more easily by truncating scales of motion rather than statistical moments, is supported by results, especially those in wall-bounded flows. But the hope that very simple eddy-viscosity models would be sufficient has not proved correct for the anisotropic SGS stresses caused by high mean field gradients, at least with a reasonable number of mesh points. Anisotropic meshes, which cause ambiguity in the definition of SGS length scales, and moderate Reynolds numbers, at which the roles of the various scales overlap, introduce additional modeling difficulties. The

decomposition of SGS stress into mean and fluctuations, which essentially models separately the SGS energy transfer from the mean flow and that from the remainder of the resolved scales, provides a workable closure for the wall-bounded cases reported. Despite the ad hoc nature of the model, it demonstrates the ability of an LES to base the SGS model on subsets of the resolved set of scales. The explicit calculation of the Leonard and "cross" terms, and the related modeling ideas of Bardina et al. (1980), also directly utilize more information from the resolved scales to reduce model error.

The nature of the flow near walls requires the expensive resolution of very small scales. The cost of resolution can be reduced by embedding a fine mesh only near the wall. However, the scale disparity between "wall" and "wake" layers, the presence of the overlap "log" layer, and the known form of the organized eddies near the wall strongly suggest that in some practical applications the wall layer can be replaced by a boundary condition for the wake layer that is imposed in the log layer. This situation is analogous to the separation at high Reynolds number of the energy-containing scales and the dissipative scales by an inertial range, and we certainly believe closure is possible in the inertial range in that case.

Inflow and outflow boundary conditions present a major obstacle in the calculation of complex engineering flows. In self-similar cases (wakes, jets, mixing layers, etc.) the use of periodic boundary conditions in the appropriate similarity coordinates seems natural, but in the more general case it will be necessary to measure the sensitivity of computed values to the inflow and outflow conditions used.

The future of turbulence simulation appears bright indeed. While there remains much work to be done on simulation technique, modeling, and numerical methods, we have already reached the point of being able to generate more information than we are able to digest. One can imagine in the near future a researcher at a graphics terminal with access to computed turbulent flow fields of high resolution. He will be able to display any desired quantity computed from the field (for example, statistical averages or three-dimensional visualizations of fluid motion and eddy structure). The computer can answer any question about the fields it holds, and the researcher can devote his time to the really difficult effort of finding the right question to ask. The experimentalist must arrange his experiment and gather the specific data needed to answer his questions; if these answers suggest other questions, the experiment must frequently be rerun to collect new data. The use of stored simulation results places fewer constraints on the questions that can be answered, and allows rapid interactive display of results. An experimentalist with access to such a data base would be able to evaluate the choices of data to be taken from the experiment; for example, he could tune a conditional sampling strategy to capture more precisely the

events of interest. A person developing turbulence models could use the data base to evaluate proposed models. Furthermore, the flow-field data base can be shared by other researchers who do not have the computer power required to generate the fields, but do have enough power to probe them. The development of hardware and software tools for interactive probing of simulation results, the availability of the computed flow fields (in computer-readable form), and the advancement in computer capacity will ultimately determine the degree to which simulation enhances our understanding and ability to control turbulence.

Literature Cited

Antonopoulos-Domis, M. 1981. Large-eddy simulation of a passive scalar in isotropic turbulence. *J. Fluid Mech.* 104: 55–79

Bardina, J., Ferziger, J. H., Reynolds, W. C. 1980. Improved subgrid-scale models for large-eddy simulation. *AIAA Pap. 80-1357*

Baron, F. 1982. *Three-dimensional large-eddy simulation of turbulent shear flows.* Doctoral thesis. Univ. Pierre Marie Curie, Paris

Blackwelder, R. F., Kaplan, R. E. 1976. On the wall structure of the turbulent boundary layer. *J. Fluid Mech.* 76: 89–112

Bull, M. K. 1967. Wall pressure fluctuations associated with subsonic turbulent boundary layer flow. *J. Fluid Mech.* 28: 719–54

Cain, A. B., Reynolds, W. C., Ferziger, J. H. 1981. A three-dimensional simulation of transition and early turbulence in a time-developing mixing layer. *Rep. TF-14*, Dept. Mech. Eng., Stanford Univ.

Cambon, C., Jeandel, D., Mathieu, J. 1981. Spectral modelling of homogeneous non-isotropic turbulence. *J. Fluid Mech.* 104: 247–62

Chapman, D. R. 1979. Computational aerodynamics development and outlook. *AIAA J.* 17: 1293–1313

Chapman, D. R. 1981. Trends and pacing items in computational aerodynamics. See Reynolds & MacCormack 1981, pp. 1–11

Chapman, D. R., Kuhn, G. D. 1981. Two-component Navier-Stokes computational model of viscous sublayer turbulence. *AIAA Pap. 81-1024*

Chollet, J. 1982. Two-point closures as a subgrid scale modeling for large eddy simulations. *NCAR Preprint 0901/82-16.* Presented at Symp. Turbul. Shear Flows, Karlsruhe, West Ger., Sept. 1983

Chollet, J., Lesieur, M. 1981. Parameterization of small scales of three-dimensional isotropic turbulence utilizing spectral closures. *J. Atmos. Sci.* 38: 2747–57

Clark, R. A., Ferziger, J. H., Reynolds, W. C. 1977. Evaluation of subgrid-scale turbulence models using a fully simulated turbulent flow. *Rep. TF-9*, Dept. Mech. Eng., Stanford Univ.

Clark, R. A., Ferziger, J. H., Reynolds, W. C. 1979. Evaluation of subgrid-scale models using an accurately simulated turbulent flow. *J. Fluid Mech.* 91: 1–16

Comte-Bellot, G. 1963. *Contribution a l'etude de la turbulence de conduite.* Doctoral thesis. Univ. Grenoble

Comte-Bellot, G., Corrsin, S. 1971. Simple Eulerian time correlation of full- and narrow-band velocity signals in grid-generated "isotropic" turbulence. *J. Fluid Mech.* 48: 273–337

Corrsin, S. 1961. Turbulent flow. *Am. Sci.* 49: 300–25

Corrsin, S. 1974. Limitations of gradient transport models in random walks and in turbulence. See Frenkiel & Munn 1974, pp. 25–60

Deardorff, J. W. 1970. A numerical study of three-dimensional turbulent channel flow at large Reynolds numbers. *J. Fluid Mech.* 41: 453–80

Deardorff, J. W. 1971. On the magnitude of the subgrid scale eddy coefficient. *J. Comput. Phys.* 7: 120–33

Deardorff, J. W. 1973. The use of subgrid transport equations in a three-dimensional model of atmospheric turbulence. *J. Fluids Eng.* 95: 429–38

Deissler, R. G. 1961. Effects of inhomogeneity and of shear flow in weak turbulence fields. *Phys. Fluids* 4: 1187–98

Deissler, R. G. 1972. Growth of turbulence in the presence of shear. *Phys. Fluids* 15: 1918–20

Durst, F., Launder, B. E., Schmidt, F. W., Whitelaw, J. H., eds. 1979. *Turbulent Shear Flows I.* Berlin: Springer. 413 pp.

Eckelmann, H. 1974. The structure of the

viscous sublayer and the adjacent wall region in a turbulent channel flow. *J. Fluid Mech.* 65:439–59

Feiereisen, W. J., Reynolds, W. C., Ferziger, J. H. 1981. Numerical simulation of compressible, homogeneous, turbulent shear flow. *Rep. TF-13*, Dept. Mech. Eng., Stanford Univ.

Ferziger, J. H. 1982. State of the art in subgrid scale modeling. In *Numerical and Physical Aspects of Aerodynamic Flows*, ed. T. Cebici, pp. 53–68. New York: Springer. 636 pp.

Ferziger, J. H., Mehta, U. B., Reynolds, W. C. 1977. *Large eddy simulation of homogeneous isotropic turbulence.* Presented at Symp. Turbul. Shear Flows, Penn. State Univ., University Park

Fox, D. G., Deardorff, J. W. 1972. Computer methods for simulation of multidimensional, nonlinear, subsonic, incompressible flows. *J. IIeat Transfer* 94:337–46

Fox, D. G., Lilly, D. K. 1972. Numerical simulation of turbulent flows. *Rev. Geophys. Space Phys.* 10:51–72

Fox, L., Parker, I. 1968. Chebyshev polynomials in numerical analysis. London: Oxford Univ. Press

Frenkiel, F. N., Munn, R. E., eds 1974. *Proc. Symp. Turbul. Diffus. Environ. Pollut., Charlottesville, 1973. Advances in Geophysics*, Vol. 18A. New York: Academic. 462 pp.

Gottlieb, D., Orszag, S. A. 1977. Numerical analysis of spectral methods: theory and application. *CBMS-NSF Reg. Conf. Ser. Appl. Math.*, Vol. 26. Philadelphia: SIAM. 170 pp.

Grotzbach, G. 1979. Numerical investigation of radial mixing capabilities in strongly buoyancy-influenced vertical, turbulent channel flows. *Nucl. Eng. Des.* 54:49–66

Grotzbach, G. 1981. Spatial resolution requirements for numerical simulation of internally heated fluid layers. In *Numerical Methods in Laminar and Turbulent Flow*, ed. C. Taylor, B. A. Schrefler, pp. 593–604. Swansea, UK: Pineridge

Grotzbach, G., Schumann, U. 1979. Direct numerical simulation of turbulent velocity-, pressure-, and temperature-fields in channel flows. See Durst et al. 1979, pp. 370–85

Harlow, F. H., Welch, J. E. 1965. Numerical calculation of time-dependent viscous incompressible flow of fluid with free surface. *Phys. Fluids* 8:2182–89

Harris, V. G., Graham, J. A. H., Corrsin, S. 1977. Further experiments in nearly homogeneous turbulent shear flow. *J. Fluid Mech.* 81:657–87

Herring, J. R., Orszag, S. A., Kraichnan, R. H., Fox, D. G. 1974. Decay of two-dimensional homogeneous turbulence. *J. Fluid Mech.* 66:417–44

Kim, H. T., Kline, S. J., Reynolds, W. C. 1971. The production of turbulence near a smooth wall in a turbulent boundary layer. *J. Fluid Mech.* 50:133–60

Kim, J. 1983. On the structure of wall-bounded turbulent flows. *NASA TM-84313.* Also *Phys. Fluids* 1983. In press

Kleiser, L., Schumann, U. 1979. Treatment of incompressibility and boundary conditions in 3-D numerical spectral simulations of plane channel flows. *Proc. GAMM Conf. Numer. Meth. Fluid Mech., 3rd*, pp. 165–73. Braunscheig/Wiesbaden: Friedr. Vieweg & Sohn

Kline, S. J., Reynolds, W. C., Schraub, F. A., Runstadler, P. W. 1967. The structure of turbulent boundary layers. *J. Fluid Mech.* 30:741–73

Kollmann, W., ed. 1980. *Prediction Methods for Turbulent Flows.* New York: Hemisphere. 468 pp.

Kraichnan, R. H. 1976. Eddy viscosity in two and three dimensions. *J. Atmos. Sci.* 33:1521–36

Krause, E., ed. 1982. *Proc. Int. Conf. Numer. Methods Fluid Dyn., 8th, Aachen. Lecture Notes in Physics*, Vol. 170. New York: Springer. 569 pp.

Kwak, D., Reynolds, W. C., Ferziger, J. H. 1975. Three-dimensional time-dependent computation of turbulent flow. *Rep. TF-5*, Dept. Mech. Eng., Stanford Univ.

Laufer, J. 1951. Investigation of turbulent flow in a two-dimensional channel. *NACA Rep. 1053*

Leonard, A. 1974. Energy cascade in large-eddy simulations of turbulent fluid flows. See Frenkiel & Munn 1974, pp. 237–48

Leonard, A. 1980. Vortex methods for flow simulation. *J. Comput. Phys.* 37:289–335

Leonard, A., Wray, A. 1982. A new numerical method for the simulation of three-dimensional flow in a pipe. See Krause 1982, pp. 335–42

Lesieur, M., Schertzer, D. 1978. Amortissement autosimilaire d'une turbulence a grand nombre de Reynolds. *J. Méc.* 17:610–46

Leslie, D. C. 1973. *Developments in the Theory of Turbulence.* Oxford: Clarendon. 368 pp.

Leslie, D. C., Quarini, G. L. 1979. The application of turbulence theory to the formulation of subgrid modelling procedures. *J. Fluid Mech.* 91:65–91

Lilly, D. K. 1964. Numerical solutions for the shape-preserving two-dimensional thermal convection element. *J. Atmos. Sci.* 21:83–98

Lilly, D. K. 1966. On the application of the eddy viscosity concept in the inertial sub-

range of turbulence. *NCAR Manuscr. 123*

Love, M. D. 1980. Subgrid modelling studies with Burgers' equation. *J. Fluid Mech.* 100:87–110

Love, M. D., Leslie, D. C. 1979. Studies of sub-grid modelling with classical closures and Burgers' equation. See Durst et al. 1979, pp. 353–69

Lumley, J. L. 1980. Second order modelling of turbulent flows. See Kollmann 1980, pp. 1–32

Mansour, N. N., Ferziger, J. H., Reynolds, W. C. 1978. Large-eddy simulation of a turbulent mixing layer. *Rep. TF-11*, Dept. Mech. Eng., Stanford Univ.

Mansour, N. N., Moin, P., Reynolds, W. C., Ferziger, J. H. 1979. Improved methods for large eddy simulations of turbulence. See Durst et al. 1979, pp. 386–401

McMillan, O. J., Ferziger, J. H. 1979. Direct testing of subgrid-scale models. *AIAA J.* 17:1340-46

McMillan, O. J., Ferziger, J. H., Rogallo, R. S. 1980. Tests of new subgrid-scale models in strained turbulence. *AIAA Pap. 80-1339*

Metcalfe, R. W., Riley, J. J. 1981. Direct numerical simulations of turbulent shear flows. See Reynolds & MacCormack 1981, pp. 279–84

Moin, P. 1982. Numerical simulation of wall-bounded turbulent shear flows. See Krause 1982, pp. 53–76

Moin, P., Kim, J. 1980. On the numerical solution of time-dependent viscous incompressible fluid flows involving solid boundaries. *J. Comput. Phys.* 35:381–92

Moin, P., Kim, J. 1982. Numerical investigation of turbulent channel flow. *J. Fluid Mech.* 118:341–77

Monin, A. S., Yaglom, A. M. 1971. *Statistical Fluid Mechanics*, Vol. 1. Cambridge, Mass: MIT Press. 769 pp.

Orszag, S. A. 1970. Analytical theories of turbulence. *J. Fluid Mech.* 41:363–86

Orszag, S. A. 1971. Numerical simulation of incompressible flows within simple boundaries: accuracy. *J. Fluid Mech.* 49:75–112

Orszag, S. A. 1972. Comparison of pseudospectral and spectral approximation. *Stud. Appl. Math.* 51:253–59

Orszag, S. A. 1980. Spectral methods for problems in complex geometries. *J. Comput. Phys.* 37:70–92

Orszag, S. A., Kells, L. C. 1980. Transition to turbulence in plane Poiseuille and plane Couette flow. *J. Fluid Mech.* 96:159–205

Orszag, S. A., Pao, Y. 1974. Numerical computation of turbulent shear flows. See Frenkiel & Munn 1974, pp. 225–36

Orszag, S. A., Patterson, G. S. 1972. Numerical simulation of three-dimensional homogeneous isotropic turbulence. *Phys. Rev. Lett.* 28:76–79

Patterson, G. S., Orszag, S. A. 1971. Spectral calculations of isotropic turbulence: efficient removal of aliasing interactions. *Phys. Fluids.* 14:2538–41

Phillips, N. A. 1959. An example of nonlinear computational instability. In *The Atmosphere and Sea in Motion*, ed. B. Bolin, pp. 501–4. New York: Rockefeller Inst. Press

Rajagopalan, S., Antonia, R. A. 1979. Some properties of the large structure in a fully developed turbulent duct flow. *Phys. Fluids* 22:614–22

Reynolds, W. C. 1976. Computation of turbulent flows. *Ann. Rev. Fluid Mech.* 8:183–208

Reynolds, W. C., MacCormack, R. W., eds. 1981. *Proc. Int. Conf. Numer. Methods Fluid Dyn., 7th, Stanford/NASA-Ames, 1980. Lecture Notes in Physics*, Vol. 141. New York: Springer. 485 pp.

Riley, J. J., Metcalfe, R. W. 1980a. Direct numerical simulations of the turbulent wake of an axisymmetric body. In *Turbulent Shear Flows II*, eds. J. S. Bradbury, F. Durst, B. E. Launder, F. W. Schmidt, J. H. Whitelaw, pp. 78–93. Berlin: Springer. 480 pp.

Riley, J. J., Metcalfe, R. W. 1980b. Direct numerical simulation of a perturbed, turbulent mixing layer. *AIAA Pap. 80-0274*

Robinson, S. K. 1982. An experimental search for near-wall boundary conditions for large eddy simulation. *AIAA Pap. 82-0963*

Rogallo, R. S. 1981. Numerical experiments in homogeneous turbulence. *NASA TM-81315*

Roshko, A. 1976. Structure of turbulent shear flows: a new look. *AIAA J.* 14:1349–57

Roy, P. 1982. Numerical simulation of homogeneous anisotropic turbulence. See Krause 1982, pp. 440-47

Schumann, U. 1975. Subgrid scale model for finite difference simulations of turbulent flows in plane channels and annuli. *J. Comput. Phys.* 18:376–404

Schumann, U., Grotzbach, G., Kleiser, L. 1980. Direct numerical simulation of turbulence. See Kollmann 1980, pp. 124–258

Shaanan, S., Ferziger, J. H., Reynolds, W. C. 1975. Numerical simulation of turbulence in the presence of shear. *Rep. TF-6*, Dept. Mech. Eng., Stanford Univ.

Shirani, E., Ferziger, J. H., Reynolds, W. C. 1981. Mixing of a passive scalar in isotropic and sheared homogeneous turbulence. *Rep. TF-15*, Dept. Mech. Eng., Stanford Univ.

Siggia, E. D. 1981. Numerical study of small-scale intermittency in three-dimensional turbulence. *J. Fluid Mech.* 107:375–406

Smagorinsky, J. 1963. General circulation experiments with the primitive equations. I. The basic experiment. *Mon. Weather Rev.* 91:99–164

Tavoularis, S., Corrsin, S. 1981. Experiments in nearly homogeneous turbulent shear flow with a uniform mean temperature gradient. Part 1. *J. Fluid Mech.* 104:311–47

Tennekes, H., Lumley, J. L. 1972. *A First Course in Turbulence.* Cambridge, Mass: MIT Press. 300 pp.

Townsend, A. A. 1976. *The Structure of Turbulent Shear Flow.* Cambridge Univ. Press. 429 pp. 2nd ed.

Warming, R. F., Hyett, B. J. 1974. The modified equation approach to the stability and accuracy analysis of finite-difference methods. *J. Comput. Phys.* 14:159–79

Willmarth, W. W. 1975. Pressure fluctuations beneath turbulent boundary layers. *Ann. Rev. Fluid Mech.* 7:13–38

Yoshizawa, A. 1979. A statistical investigation upon the eddy viscosity in incompressible turbulence. *J. Phys. Soc. Jpn.* 47:1665–69

Yoshizawa, A. 1982. A statistically-derived subgrid model for the large-eddy simulation of turbulence. *Phys. Fluids.* 25:1532–38